MicroRNA-214 Promotes Dendritic Development by Targeting the Schizophrenia-associated Gene Quaking (Qki)

入江, 浩一郎

https://doi.org/10.15017/1806918

出版情報：九州大学, 2016, 博士（医学）, 課程博士
バージョン：

THE JOURNAL OF BIOLOGICAL CHEMISTRY VOL. 291, NO. 26, pp. 13891–13904, June 24, 2016

MicroRNA-214 Promotes Dendritic Development by Targeting the Schizophrenia-associated Gene Quaking (*Qki*)*

Received for publication, November 24, 2015, and in revised form, April 27, 2016 Published, JBC Papers in Press, April 28, 2016, DOI 10.1074/jbc.M115.705749

Koichiro Irie, Keita Tsujimura[1], Hideyuki Nakashima, and Kinichi Nakashima[2]

From the Department of Stem Cell Biology and Medicine, Graduate School of Medical Sciences, Kyushu University, 3-1-1 Maidashi, Higashi-ku, Fukuoka, Fukuoka 812-8582, Japan

Proper dendritic elaboration of neurons is critical for the formation of functional circuits during brain development. Defects in dendrite morphogenesis are associated with neuropsychiatric disorders, and microRNAs are emerging as regulators of aspects of neuronal maturation such as axonal and dendritic growth, spine formation, and synaptogenesis. Here, we show that miR-214 plays a pivotal role in the regulation of dendritic development. Overexpression of miR-214 increased dendrite size and complexity, whereas blocking of endogenous miR-214-3p, a mature form of miR-214, inhibited dendritic morphogenesis. We also found that miR-214-3p targets quaking (*Qki*), which is implicated in psychiatric diseases such as schizophrenia, through conserved target sites located in the 3′-untranslated region of *Qki* mRNA, thereby down-regulating Qki protein levels. Overexpression and knockdown of *Qki* impaired and enhanced dendritic formation, respectively. Moreover, overexpression of *Qki* abolished the dendritic growth induced by miR-214 overexpression. Taken together, our findings reveal a crucial role for the miR-214-Qki pathway in the regulation of neuronal dendritic development.

Neurons are highly polarized cells composed of the following two structurally and functionally distinct processes: the axon, which relays information to other neurons, and the dendrites, which receive information inputs from other neurons (1). The dendrites are the primary site in neurons where synapse formation and signal integration occur, with dendrite size and the extent of arborization determining the number and distribution of innervating axons and functional synapses (2, 3). Because dendrites play a critical role in defining the synaptic input, regulation of their growth is profoundly important for the establishment of functional neuronal networks (4, 5). Consequently, impaired dendritic growth is associated with a broader class of neurodevelopmental disorders, including psychiatric diseases (6). However, the mechanisms governing dendritic growth remain to be fully elucidated.

MicroRNAs (miRNAs)[3] are small noncoding RNAs that function as modulators of gene expression at the post-transcriptional level and thereby influence many biological processes, including cellular proliferation, differentiation, and apoptosis. Primary miRNAs (pri-miRNAs) are transcribed from DNA and are processed into precursor miRNAs (pre-miRNAs) by the Drosha complex in the nucleus. The pre-miRNAs are transported from the nucleus to cytoplasm and are processed into mature miRNAs by Dicer. Mature miRNAs bind to the 3′-untranslated region (3′UTR) of target mRNAs and negatively regulate gene expression by inhibiting translation or mRNA degradation (7, 8). Recent studies have shown that miRNAs act as regulators of neurodevelopment and dysregulation, which may contribute to neurological disorders (9, 10). For example, miR-9 negatively regulates axonal growth and branching by targeting microtubule-associated protein 1b mRNA (11), and miR-138 restricts the size of dendritic spines through the regulation of acyl protein thioesterase 1 (12), whereas miR-137 inhibits dendritic morphogenesis by regulating the level of Mind bomb1 protein translation (13).

miR-214 functions in various cell types, promoting myogenic differentiation of C2C12 cells by targeting N-*ras* (14) and up-regulating the expression level of Nanog by targeting *p53* to regulate ovarian cancer cell stemness (15). miR-214 has also been shown to act as a regulator of cardiomyocyte Ca^{2+} homeostasis and survival (16) and to promote neurite outgrowth during differentiation of neuroblastoma cells (17). However, the role of miR-214 in neuronal development remains elusive.

In this study, we show that miR-214 plays a key role in dendritic morphogenesis of hippocampal neurons. Overexpression and blocking of miR-214 promoted and inhibited dendrite development, respectively. In addition, we identified the mRNA of the quaking gene, called quaking homolog, KH domain RNA binding (*Qki*), which is implicated in psychiatric disorders (18, 19), as a direct target of miR-214-3p. Furthermore, we show that Qki perturbs dendrite formation and that Qki expression abolishes the dendritic phenotypes caused by miR-214 overexpression. These findings reveal a critical role for the miR-214-Qki pathway in the regulation of neuronal development.

* This work was supported in part by a Grant-in-aid for Scientific Research (A) 24240051, a grant-in-aid for scientific research on innovative areas: Foundation of Synapse and Neurocircuit Pathology, and Intramural Research Grant 27-7 for Neurological and Psychiatric Disorders of the National Center of Neurology and Psychiatry. The authors declare that they have no conflicts of interest with the contents of this article.

[1] To whom correspondence may be addressed: Dept. of Cell Pharmacology, Nagoya University Graduate School of Medicine, 65 Tsurumai, Showa, Nagoya 466-8550, Japan. Tel.: 81-52-744-2076; Fax: 81-52-744-2083; E-mail: tsujimura@med.nagoya-u.ac.jp.

[2] To whom correspondence may be addressed. Tel.: 81-92-642-6196; Fax: 81-92-642-6561; E-mail: kin1@scb.med.kyushu-u.ac.jp.

[3] The abbreviations used are: miRNA, microRNA; ANOVA, analysis of variance; qRT, quantitative RT; DIV, day *in vitro*; pri-miRNA, primary miRNA; pre-miRNA, precursor miRNA; Fw, forward; Rv, reverse.

Experimental Procedures

Animals—All aspects of animal care and treatment were carried out according to the guidelines of the Experimental Animal Care Committee of Kyushu University. Timed-pregnant ICR mice (Japan SLC) were used in this research.

Cell Culture—Hippocampal neuronal cultures were established as described previously (20). Briefly, hippocampi were dissected from embryonic day 17.5 (E17.5) mice and were digested in S-MEM (Gibco) containing 0.1% papain (Sigma) and triturated with 60 mg/ml DNase I (Sigma) and 10% fetal bovine serum (FBS). Dissociated cells were plated on poly-L-lysine (10 μg/ml, Sigma)-coated culture dishes at densities of 1×10^4 cells/cm^2 and 5×10^4 cells/cm^2 for immunocytochemistry and immunoblotting, respectively. When neurons had adhered (after 3–4 h), the medium was replaced with serum-free neuronal maintenance medium, consisting of Neurobasal (Invitrogen) medium supplemented with B27 (Invitrogen) and 0.5 mM GlutaMAX (Invitrogen). Cytosine β-D-arabinofuranoside hydrochloride (Sigma) was added 1 day after plating to eliminate proliferating undifferentiated and glial cells. The medium was changed every 3 days. HEK293T cells were cultured in DMEM containing 10% FBS and gentamicin (Nacalai Tesque).

Construction of Vectors—Lentivirus vectors used to express short hairpin RNA for *Qki* (pLLX-shQki) and FLAG-tagged Qki (pLEMPRA-Qki and pLEMPRA-Qki-3′UTR) were generously provided by Drs. Z. Zhou and M. E. Greenberg. pLLX and pLEMPRA are dual-promoter lentivirus vectors constructed by inserting the U6 promoter-driven shRNA cassette 5′ into the ubiquitin-C promoter in the FUIGW plasmid (21, 22). Plasmid pLLX-primary-miR-214 was constructed by inserting a PCR-amplified fragment from mouse genomic DNA into the HpaI and XhoI sites of pLLX. shRNA for *Qki* and sponges against miR-214–5p- or -3p-expressing lentivirus plasmids were constructed by inserting the following oligonucleotides into the HpaI and XhoI sites of pLLX: sh-Qki-1-Fw, 5′-tCCCTACCATAATGCCTTTGATttcaagagaATCAAAGGCATTATGGTAGGGttttttttgaac-3′, and sh-Qki-1-Rv, 5′-tcgagttccaaaaaaCCCTACCATAATGCCTTTGATtctcttgaaATCAAAGGCATTATGGTA-3′; sh-Qki-2-Fw, 5′-tGACGAAGAAATTAGCAGAGTAttcaagagaTACTCTGCTAATTTCTTCGTCttttttttgaac-3′, and sh-Qki-2-Rv, 5′-tcgagttccaaaaaaGACGAAGAAATTAGCAGAGTAtctcttgaaTACTCTGCTAATTTCTTCGTCa-3′; sh-Qki-3-Fw, 5′-tGGACTTACAGCTAAACAACTTttcaagagaAAGTTGTTTAGCTGTAAGTCCttttttttgaac-3′, and sh-Qki-3-Rv, 5′-tcgagttccaaaaaaGGACTTACAGCTAAACAACTTttctcttgaaAAGTTGTTTAGCTGTAAGTCCa-3′; sponge-miR-214–5p-Fw, 5′-gacgttaacGCACAGCAATGACAGACAGGCAGCACAGCAATGACAGACAGGCAGCACAGCAATGACAGACAGGCAttttttctcgaggtc, and sponge-miR-214–5p-Rv, 5′-gacctcgagaaaaaaTGCCTGTCTGTCATTGCTGTGCTGCCTGTCTGTCATTGCTGTGCTGCCTGTCTGTCATTGCTGTGCgttaacgtc-3′; sponge-miR-214-3p-Fw, 5′-gacgttaacACTGCCTGTAGTCGCCTGCTGTACTGCCTGTAGTCGCCTGCTGTACTGCCTGTAGTCGCCTGCTGTttttttctcgaggtc-3′, and Sponge-miR-214-3p-Rv, 5′-gacctcgagaaaaaaACAGCAGGCGACTACAGGCAGTACAGCAGGCGACTACAGGCAGTACAGCAGGCGACTACAGGCAGTgttaacgtc-3′. *Qki, Nptxr, Crkl, Hdgf,* and *Ldoc1* cDNA fragments and their 3′UTR-containing fragments were amplified by PCR using KOD polymerase (Toyobo) and subsequently cloned into the EcoRI and AscI sites of pLEMPRA-MeCP2 (22). The luciferase reporter plasmids pmir-GLO-Qki-3′UTR-nat, pmir-GLO-Crkl-3′UTR-nat, and pmir-GLO-Hdgf-3′UTR-nat were constructed by inserting the genomic DNA fragments of *Qki* 3′UTR (+1 to +2452), *Crkl* 3′UTR (+1 to +2000), and *Hdgf* 3′UTR (+1 to +1224) into the PmeI and XhoI sites of pmir-GLO (Promega). The each mutated luciferase reporter construct was obtained by inserting the mutated 3′UTR of *Qki*, *Crkl* and *Hdgf* with the seed regions of miR-214 into the PmeI and XhoI sites of pmir-GLO.

Lentivirus Production—Lentiviruses were produced as described previously (23). Briefly, lentiviruses were generated by co-transfecting HEK293T cells with the lentivirus vector constructs pCMV-VSV-G-RSV-Rev and pCAG-HIVgp using polyethyleneimine (Polysciences). The culture supernatants were collected 48 h after transfection, and virus was introduced into neurons by adding these supernatants to the culture media.

In Utero Electroporation—To evaluate dendritic growth *in vivo*, *in utero* electroporation was performed on E14 mouse embryos as described previously (24). Briefly, plasmid DNA (0.1 μg/μl in PBS containing 0.1% Fast-Green) was injected (0.5–1 μl) into the lateral ventricle of the embryonic brain from outside the uterus with a glass micropipette (GD-1, Narishige). Holding the embryo in the uterus with forceps-type electrodes (NEPA GENE), 50-ms electric pulses of 45 V were delivered five times at intervals of 950 ms using a model CUY21 Single Cell Electroporator (Nepa Gene). Glass micropipettes were prepared using a P-1000IVF (Sutter). Animals were perfused with 4% paraformaldehyde at postnatal day 10 (P10). Collected brains were postfixed with 4% paraformaldehyde overnight at 4 °C and then equilibrated in 30% sucrose. Brains were frozen at −80 °C after embedding in optimal cutting temperature compound (Sakura Finetek) and serially sectioned at 40-μm thickness.

Immunocytochemistry—Cells were fixed at the indicated day(s) *in vitro* (DIV) with 4% paraformaldehyde in phosphate-buffered saline (PBS), washed with PBS, permeabilized, and blocked with blocking buffer (3% FBS and 0.1% Triton X-100 in PBS) at room temperature. The cells were then incubated with primary antibody solution at room temperature for 3 h. After being washed with PBS, the cells were incubated with secondary antibody solution at room temperature for 1 h, and after further washing with PBS, they were mounted on glass slides.

Immunohistochemistry—Sections were washed with PBS, permeabilized, and blocked with blocking buffer at room temperature. The sections were incubated with primary antibody solution overnight at 4 °C. After being washed with PBS, the sections were incubated with secondary antibody solution at room temperature for 2 h. After being washed with PBS, the sections were mounted on glass slides. Fluorescence images were acquired using a Zeiss LSM 700 confocal microscope with a ×20 objective lens. Z series of 20 images were taken at 1-μm intervals at a 1024 × 1024-pixel resolution.

Immunoblotting—Cells were lysed with a buffer containing 0.5% Nonidet P-40, 10 mM Tris-HCl, pH 7.5, 150 mM NaCl, and 1% protease inhibitor mixture (Nacalai Tesque). Lysates were sonicated and centrifuged at 20,000 × *g* for 15 min at 4 °C. Total cell lysates were subjected to SDS-PAGE and transferred to a PVDF transfer membrane (GE Healthcare). The blots were blocked with 0.3% skim milk in TBST (50 mM Tris-HCl, pH 7.5, 150 mM NaCl, 0.1% Tween 20), and after incubation with a primary antibody, they were washed with TBST and incubated with a peroxidase-conjugated secondary antibody. Immunoreactive bands were detected by enhanced chemiluminescence using ECL Prime Western blotting detection reagent (GE Healthcare).

Antibodies—For immunocytochemistry and immunohistochemistry, the following primary antibodies were used: chicken anti-green fluorescent protein (GFP) (1:1000; Aves Labs); guinea pig anti-microtubule-associated protein 2 (MAP2) (1:1000; Synaptic Systems); mouse anti-Tau-1 (1:1000; Millipore); and rabbit anti-β-III tubulin (Tuj-1) (1:1000; Covance). The following secondary antibodies were used: CF488A donkey anti-chick IgY (IgG) (H + L) highly cross-adsorbed (1:500; Biotium); CF555 donkey anti-guinea pig IgG (H + L) highly cross-adsorbed (1:500; Biotium); CF555 donkey anti-rabbit IgG (H + L) highly cross-adsorbed (1:500; Biotium); and CF647 donkey anti-mouse IgG (H + L) highly cross-adsorbed (1:500; Biotium). Nuclei were stained using bisbenzimide H33258 fluorochrome trihydrochloride (Nacalai Tesque).

For immunoblotting, the following primary antibodies were used: rabbit anti-QKI (1:250; Proteintech) and mouse anti-β-actin (1:1000; Cell Signaling Technology). The following secondary antibodies were used: anti-mouse IgG, HRP-linked whole antibody from sheep (1:5000; GE Healthcare), and anti-rabbit IgG, HRP-linked whole antibody from donkey (1:5000; GE Healthcare).

Luciferase Reporter Assay—Hippocampal neurons were co-transfected with control (pLLX) or miR-214 expression vector and pmir-GLO-Qki-3′UTR-nat, pmir-GLO-Qki-3′UTR-mut, pmir-GLO-Crkl-3′UTR-nat, pmir-GLO-Crkl-3′UTR-mat, pmir-GLO-Hdgf-3′UTR-nat, or pmir-GLO-Hdgf-3′UTR-mat using Lipofectamine 2000 (Life Technologies, Inc.). After transfection, the cells were incubated for 3 days and lysed with Reporter Lysis Buffer. Luciferase activity of the lysates was measured with the Dual-Glo Luciferase Assay System (Promega) according to the manufacturer's protocol. Firefly luciferase activities were determined by three independent transfections and normalized by comparison with the *Renilla* luciferase activities of the internal control.

Morphological Analysis of Cultured Hippocampal Neurons—For analysis of neurite development, hippocampal neurons were subjected to immunocytochemistry using anti-Tuj-1 and anti-GFP antibodies at 3DIV. Tuj-1-positive neurite length was measured using ImageJ software.

To analyze axon development, hippocampal neurons were subjected to immunocytochemistry using anti-Tau-1 and anti-GFP antibody at 3DIV. Neurites with a strong Tau-1 signal at their proximal end were counted as axons. Axon length and branch number were measured using ImageJ.

For analysis of dendrite development *in vitro*, hippocampal neurons were subjected to immunostaining with antibodies against MAP2 and GFP at 6DIV. Dendrites were defined as MAP2-positive neurites. Sholl analysis and quantification of dendritic length and branch number were performed using ImageJ software. For Sholl analysis, concentric circles having 10-μm increments in radius were defined from the center of the cell body. The number of MAP2-positive dendrites crossing each circle was counted. The total number of crossings for each cell was measured as an index for total dendritic complexity as described previously (25).

For *in vivo* dendrite analysis, brain sections were subjected to immunohistochemistry with anti-GFP antibody. Total dendritic length and branch number of GFP-positive neurons in layer 4 were measured using ImageJ. For Sholl analysis, concentric circles having 10-μm increments in radius were defined from the center of the cell body. The number of GFP-positive dendrites crossing each circle was counted. The total number of crossings for each cell was calculated as an objective measurement of total dendritic complexity.

qRT-PCR—qRT-PCR analysis was performed to measure the expression levels of primary and mature miRNAs, as described previously (26). In brief, total RNAs were extracted with TRIzol (Invitrogen) and subjected to reverse transcription with the SuperScript VILO cDNA synthesis kit (Invitrogen) according to the manufacturer's protocol. qRT-PCR was performed with the StepOne real time PCR system (Applied Biosystems). To detect primary and mature miRNAs, a TaqMan microRNA assay kit (Applied Biosystems) was used in accordance with the manufacturer's protocol. Data analysis was performed using the comparative Ct method. Results were normalized to *Gapdh* or *U6* snRNA.

Statistical Analysis—The results presented are the average of at least three experiments, each performed in triplicate, with standard errors. Statistical analyses were performed by one-way ANOVA, followed by Tukey's multiple comparison tests or by Student's *t* test, as appropriate, using Prism 5 (GraphPad Software). Probabilities of $p < 0.05$ were considered significant.

Results

Structure and Expression of miR-214—miR-214 is an intragenic microRNA encoded in the mouse *dynamin 3* (*Dnm3*) gene, located on the opposite strand in the 14th intronic region (14). miR-214 is transcribed together with miR-199a-2 as an antisense RNA of *Dnm3* (*Dnm3os*) on mouse chromosome 1, and the two mature forms of miR-214, miR-214–5p and miR-214-3p, are highly conserved across mammalian species (Fig. 1*A*). To explore possible roles of miR-214 in neuronal development, we first investigated expression levels of miR-214 in the mouse brain by qRT-PCR analysis. Although regional variation was observed, substantial expression of miR-214 was confirmed in P1 mouse brain (Fig. 1*B*). We also measured the level of miR-214 in developing cultured neurons derived from E17.5 hippocampi. The expression level of primary miR-214 transiently increased at an early stage in cultured hippocampal neurons and then declined at later stages (Fig. 1*C*). However, mature miR-214 levels gradually increased during neuronal

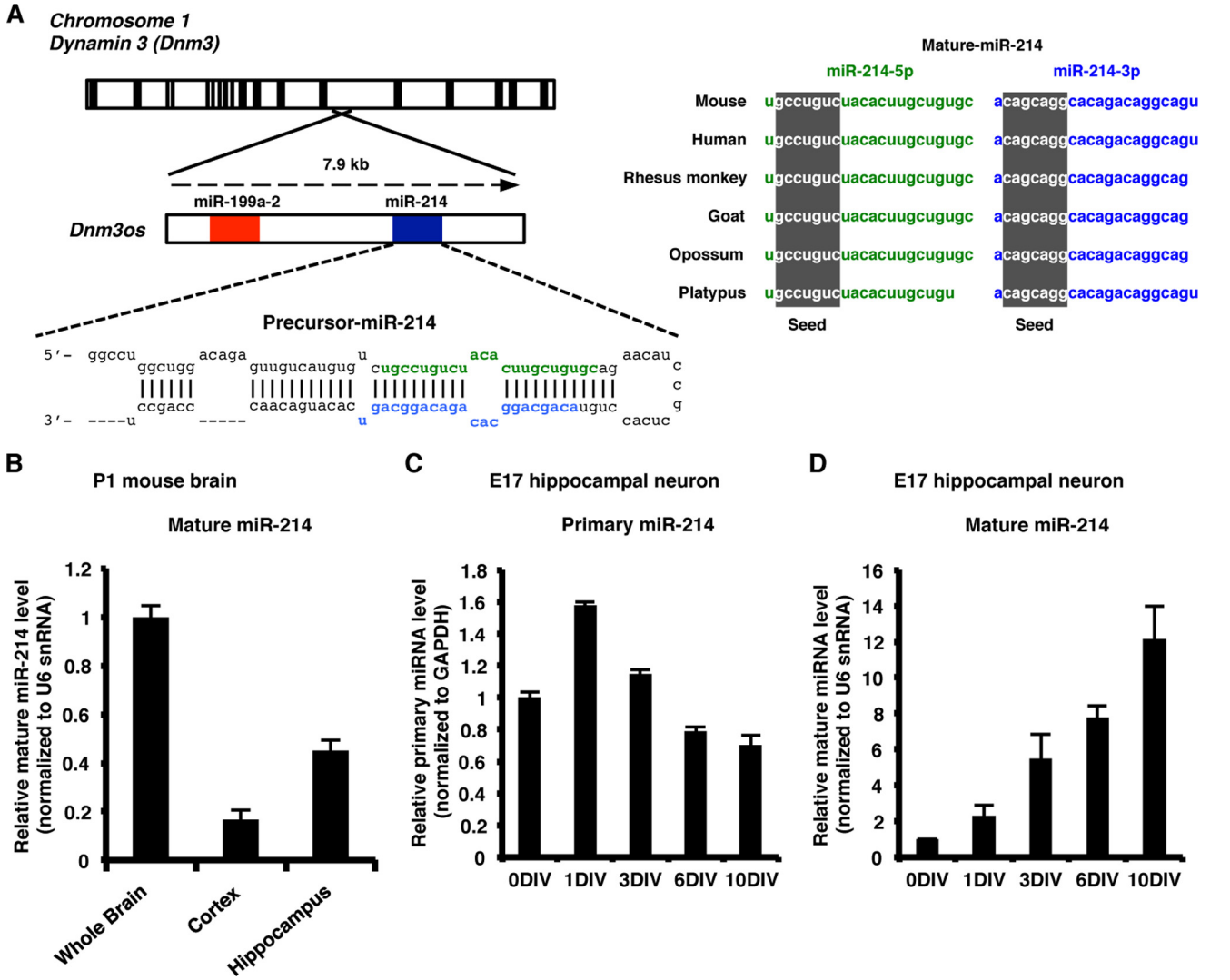

FIGURE 1. **Genomic structure of miR-214 and its expression patterns in the developing brain and hippocampal neurons.** *A*, diagram of the structure of the mouse miR-214 locus and the sequence of miR-214 precursor. pri-miR-214 is transcribed as an antisense RNA of dynamin-3 (*Dnm3os*) with pri-miR-199a-2. The nucleotide sequences of mature miR-214–5p and -3p are highly conserved among mammalian species. *Highlighted regions* indicate the seed sequence. *B*, mature miR-214 expression levels in P1 mouse brain tissues were measured by qRT-PCR. *C* and *D*, expression levels of primary (*C*) and mature (*D*) forms of miR-214 were measured by qRT-PCR in cultured developing hippocampal neurons at 0, 1, 3, 6, and 10DIV.

maturation (Fig. 1*D*), suggesting that miR-214 plays some role in neuronal development.

miR-214 Promotes Dendritic Development of Hippocampal Neurons—To investigate the function of miR-214 in neurons, we next expressed miR-214 in primary cultured E17 hippocampal neurons by infecting them with lentiviruses expressing GFP as control or GFP together with miR-214 (Fig. 2*A*), and we evaluated axonal and dendritic morphologies. Overexpression of miR-214 was confirmed by qRT-PCR (Fig. 2*B*). We found that overexpression of miR-214 in hippocampal neurons significantly increased total dendrite length and dendritic branch numbers compared with control (Fig. 2, *C–E*). We also performed Sholl analysis by measuring the number of dendrites that intersect concentric circles at different radial distances from the cell body (Fig. 2*F*). The results revealed that miR-214-expressing neurons exhibited enhanced dendritic complexity compared with control neurons (Fig. 2*G*). In accordance with this result, the total crossing number was significantly increased by miR-214 overexpression in neurons (Fig. 2*H*). However, miR-214-expressing neurons did not show any significant change in axonal growth (Fig. 2, *I* and *J*). These results suggest that miR-214 promotes dendritic but not axonal development in hippocampal neurons.

miR-214-3p Functions in Dendritic Development—Precursor miR-214 generates two mature miRNAs, miR-214–5p and miR-214-3p. Therefore, we next examined which mature form of miR-214 regulates dendritic development of neurons. We expressed an miRNA inhibitor (sponge) against each miR-214–5p and miR-214-3p (Fig. 3*A*) in hippocampal neurons and evaluated dendrite formation. Blocking of endogenous miR-214-3p significantly decreased both dendritic branch number and length compared with control, although the inhibition of miR-214–5p did not affect dendritic development (Fig. 3, *B–D*). Moreover, inhibition of miR-214-3p but not miR-214–5p markedly reduced dendritic complexity compared with control (Fig. 3, *E* and *F*). We obtained almost the same

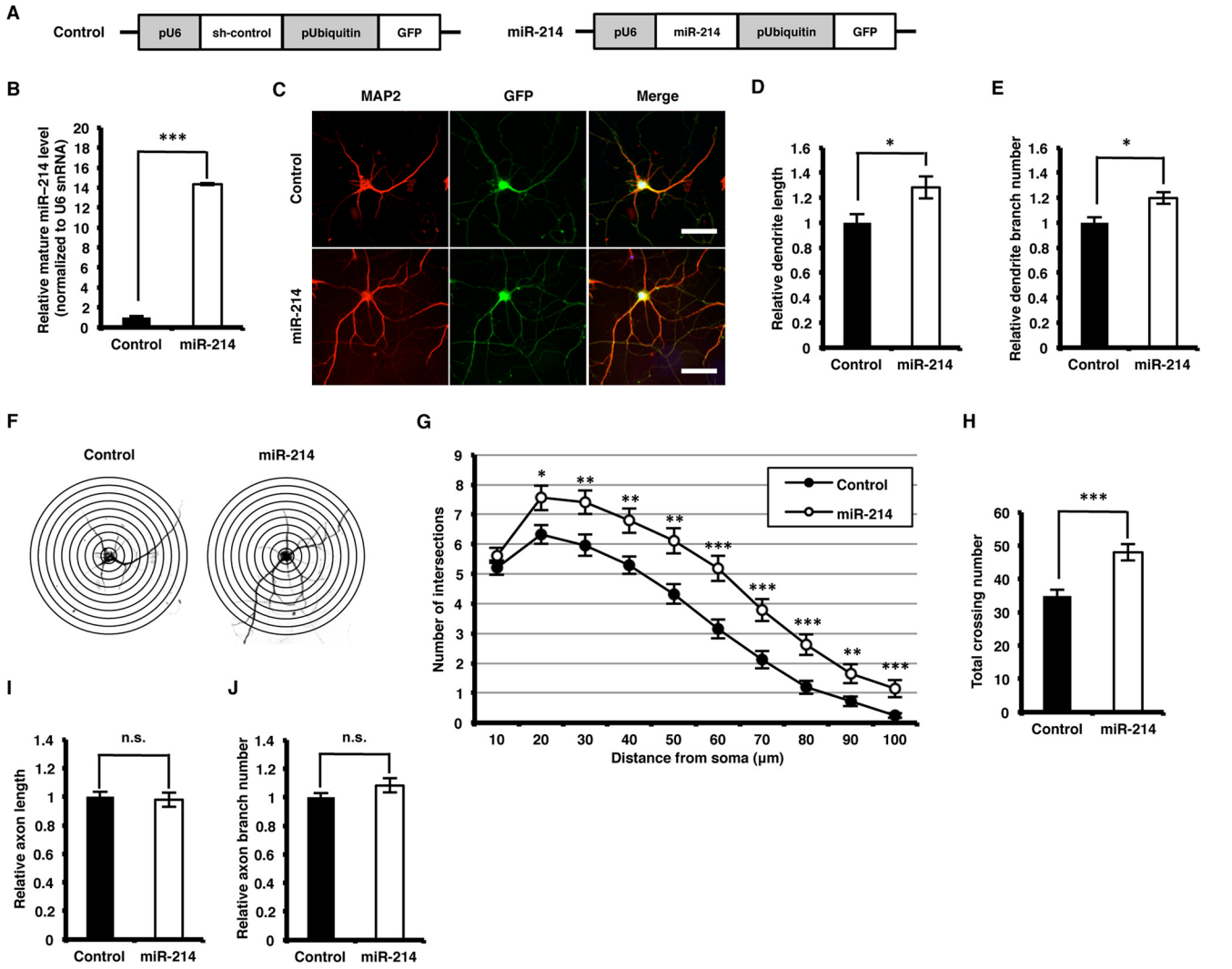

FIGURE 2. **miR-214 promotes dendritic development of cultured hippocampal neurons.** *A*, diagrams of lentiviral vector constructs. miR-214 is expressed as a short hairpin under the U6 RNA polymerase III promoter, and GFP is expressed under the ubiquitin promoter. *B*, expression levels of miR-214 were measured by qRT-PCR in hippocampal neurons infected with lentiviruses expressing miR-214. Student's *t* test, ***, $p < 0.001$. $n = 3$ independent experiments. *C*, representative images of hippocampal neurons, stained with anti-MAP2 (*red*) and anti-GFP (*green*) antibodies at 6DIV. *Scale bars*, 50 μm. *D* and *E*, quantification of total dendrite length (*D*) and dendrite branch number (*E*) in *C*. Student's *t* test, *, $p < 0.05$. $n = 4$ independent experiments; at least 50 neurons were analyzed in each experiment. *F*, representative images of neurons subjected to Sholl analysis. *G*, quantification of dendrite complexity by Sholl analysis of neurons infected with lentiviruses expressing miR-214 at 6DIV, as described in *C*. Student's *t* test, *, $p < 0.05$; **, $p < 0.01$; ***, $p < 0.001$. 50 neurons were analyzed in each condition. *H*, histogram of total number of crossings for miR-214-expressing neurons. Student's *t* test, ***, $p < 0.001$. *I* and *J*, quantification of total axon length (*I*) and axon branch number (*J*) in hippocampal neurons at 3DIV. Hippocampal neurons were infected with lentiviruses expressing only GFP or GFP together with miR-214 and immunostained for Tau-1 and GFP at 3 days after lentivirus infection. Total length and branch number of Tau-1-positive axons were measured. Student's *t* test, *n.s.*, not significant. $n = 3$ independent experiments; at least 100 neurons were analyzed in each experiment.

results by using another inhibitor for miR-214-3p with a different sequence from Sponge-miR-214-3pi-1 (data not shown). Consistent with the gain-of-function experiments, inhibition of neither miR-214–5p nor miR-214-3p influenced axonal growth (Fig. 3, *G* and *H*). These results indicate that miR-214-3p is important for dendritic development in hippocampal neurons.

miR-214-3p Targets Qki in Hippocampal Neurons—To gain further insight into the mechanisms by which miR-214 regulates dendritic development, we attempted to identify downstream target genes of miR-214-3p. We first searched miR-214-3p targets using the public databases miRDB, TargetScan, and PicTar, and 24 candidate target genes, common to all three databases, were identified. To further narrow down plausible target genes, we sought candidate targets that have more than three putative miR-214-3p seed sites in their 3′UTR and found that five genes, quaking (*Qki*), neuronal pentraxin receptor (*Nptxr*), v-*crk* avian sarcoma virus CT10 oncogene homolog-like (*Crkl*), hepatoma-derived growth factor (*Hdgf*), and leucine zipper, down-regulated in cancer 1 (*Ldoc1*), met this criterion (Fig. 4*A*). We then performed functional screening for direct miR-214-3p targets by expressing the five genes in hippocampal neurons and evaluating neurite outgrowth after 3 days. To function as a mediator of miR-214-dependent effects on dendritic formation, a downstream target of miR-214-3p should negatively regulate neurite growth. Among the candidate genes, we found that only Qki overexpression significantly suppressed Tuj-1-positive neurite outgrowth (Fig. 4, *B* and *C*). To

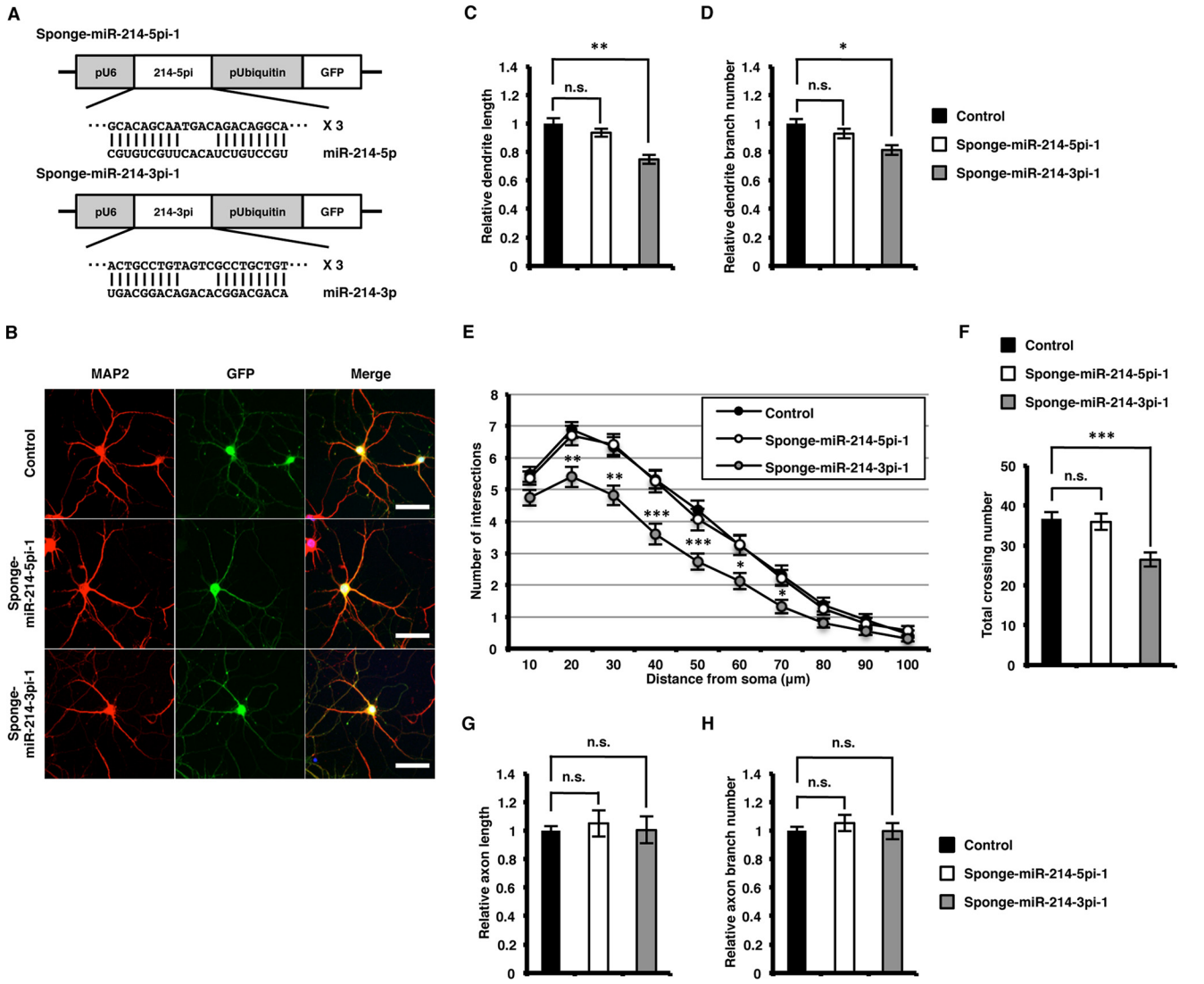

FIGURE 3. **miR-214-3p is required for dendritic development in hippocampal neurons.** *A*, diagrams of lentiviral vector constructs expressing sponges against miR-214–5p and -3p. The sponges were expressed under the U6 RNA polymerase III promoter, although GFP is expressed under the ubiquitin promoter. *B*, representative images of hippocampal neurons, stained with anti-MAP2 (*red*) and anti-GFP (*green*) antibodies at 6DIV. *Scale bars,* 50 μm. *C* and *D*, quantification of total dendrite length (*C*) and dendrite branch number (*D*) in *B*. One-way ANOVA, Tukey's post-test, *, $p < 0.05$; **, $p < 0.01$; *n.s.,* not significant. $n = 3$ independent experiments; at least 50 neurons were analyzed in each experiment. *E*, quantification of dendrite complexity by Sholl analysis of neurons infected with lentiviruses expressing sponge against miR-214–5p or -3p at 6DIV. One-way ANOVA, Tukey's post-test, *, $p < 0.05$; **, $p < 0.01$; ***, $p < 0.001$. 50 neurons were analyzed in each condition. *F*, histogram of total number of crossing for sponges against miR-214–5p- or miR-214-3p-expressing neurons. One-way ANOVA, Tukey's post-test, ***, $p < 0.001$; *n.s.,* not significant. *G* and *H*, quantification of total axon length (*G*) and axon branch number (*H*) in hippocampal neurons at 3DIV. Hippocampal neurons were infected with lentiviruses expressing sponge against miR-214–5p or -3p and immunostained for Tau-1 and GFP at 3 days after lentivirus infection. Total length and branch number of Tau-1-positive axons were measured. One-way ANOVA, Tukey's post-test, *n.s.,* not significant. $n = 3$ independent experiments; at least 100 neurons were analyzed in each experiment.

further investigate whether miR-214-3p targets *Qki* in neurons, we generated miRNA reporter constructs in which a luciferase reporter gene was placed under post-transcriptional control of the native *Qki* 3′UTR or of a *Qki* 3′UTR harboring mutations in all three miR-214-3p seed sites (Fig. 4*D*). These luciferase constructs were co-transfected with a miR-214-expressing plasmid into hippocampal neurons, and luciferase activity was measured 3 days later. The luciferase activity of the native *Qki* 3′UTR construct was significantly decreased by miR-214 expression, whereas the reporter constructs with mutated seed sequences showed no such sensitivity to miR-214 expression (Fig. 4*E, left*). In contrast, when we performed luciferase assay using the construct with 3′UTRs of *Crkl* and *Hdgf*, the luciferase activities were not altered by miR-214 expression, suggesting that mRNAs of them are not targets of miR-214 (Fig. 4*E, middle* and *right*). To determine whether miR-214 regulates expression levels of *Qki*, we expressed miR-214 and assessed Qki protein levels in neurons by immunoblotting analysis. The *Qki* gene generates three alternatively spliced isoforms encoding Qki-5, Qki-6, and Qki-7 that differ in their C-terminal 30 amino acids (27). We found that protein levels of all Qki isoforms were significantly decreased in miR-214-overexpressing cells (Fig. 4, *F* and *G*). From these observations, we concluded that miR-214-3p directly targets *Qki* in hippocampal neurons.

Overexpression of Qki Suppresses Dendritic Formation—Qki is an RNA-binding protein belonging to the STAR (signal transduction and activation of RNA) protein family, and it post-

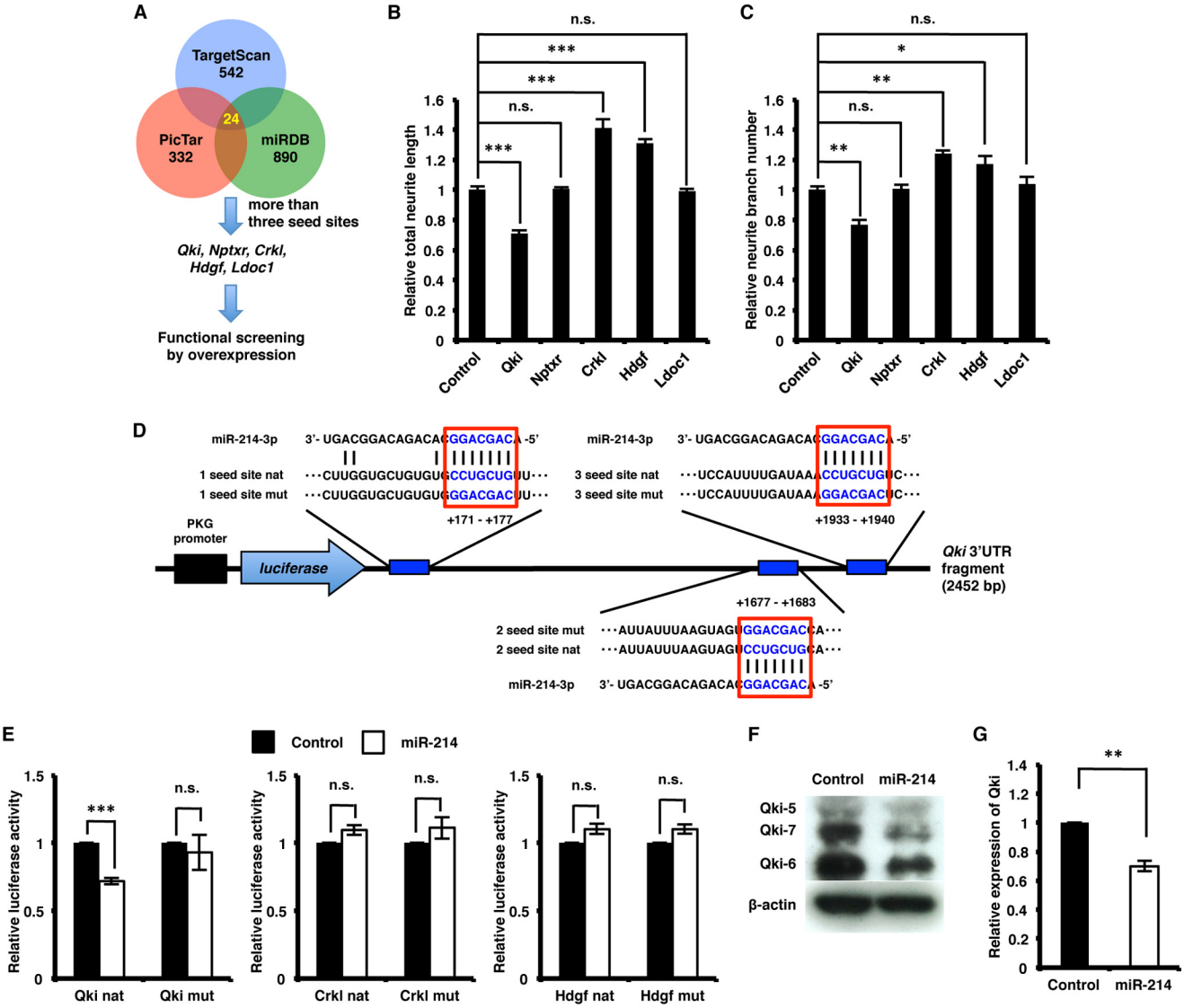

FIGURE 4. **miR-214-3p targets the *qki* 3′UTR in hippocampal neurons.** *A*, flow chart of screening for downstream targets of miR-214-3p. *B* and *C*, quantification of total neurite length (*B*) and neurite branch number (*C*) in treated hippocampal neurons at 3DIV. Hippocampal neurons were infected with lentivirus expressing only GFP (control), Qki, Nptxr, Crkl, Hdgf, or Ldoc1 and immunostained using anti-GFP and anti-β-III tubulin (Tuj-1) antibodies at 3 days after lentivirus infection. Total length and branch number of Tuj-1-positive neurites were measured. One-way ANOVA, Tukey's post-test, *, $p < 0.05$; **, $p < 0.01$; ***, $p < 0.001$; *n.s.*, not significant. $n = 3$ independent experiments; at least 50 neurons were analyzed in each experiment. *D*, luciferase reporter assays of the predicted miR-214-3p target gene *Qki*. Luciferase constructs are illustrated, showing the miR-214-3p sequence, and the miR-214-3p target sequence of native type (*nat*) and its mutated sequence (*mut*). The 5′ seed sequences of miR-214-3p are marked by *red boxes*. *E*, luciferase activity of *Qki* 3′UTR was suppressed by miR-214 overexpression at 3 days after transfection (*left*). Luciferase activity of *Crkl*- (*middle*) or *Hdgf*-3′UTR (*right*) was not altered by the expression of miR-214. Student's *t* test, ***, $p < 0.001$; *n.s.*, not significant. $n = 3$ independent experiments. *F*, Western blotting analysis showing that the levels of all three isoforms of Qki protein were decreased in miR-214-overexpressing neurons at 6DIV. *G*, quantification of total Qki protein level in *F*. Student's *t* test, **, $p < 0.01$. $n = 3$ independent experiments.

transcriptionally regulates its mRNA ligands (28). Functional studies of mouse *Qki* have revealed its role in oligodendrocyte development (28). In humans, *QKI* is located in a previously identified schizophrenia susceptibility locus on chromosome 6 (29–33). Furthermore, other studies showed reduced *QKI* expression in psychiatric diseases such as schizophrenia (34–36) and major depressive disorders (37), suggesting that QKI has an important role in the pathogenesis of psychiatric disorders, especially of schizophrenia. However, the function of QKI in neurons remains unexplored.

As a first step toward understanding the function of Qki in neurons, we performed a gain-of-function experiment by expressing Qki in hippocampal neurons (Fig. 5*A*) and evaluating dendritic growth. Overexpression of Qki was confirmed by immunoblotting using an anti-QKI antibody (Fig. 5*B*). In Qki-overexpressing neurons, total dendrite length and branch numbers decreased compared with control neurons (Fig. 5, *C*–*E*). In addition, Sholl analysis indicated that overexpression of Qki reduced the dendritic arborization of neurons (Fig. 5, *F* and *G*). These results indicate that Qki negatively regulates dendritic formation in hippocampal neurons.

Knockdown of Qki Promotes Dendritic Formation—In light of the above results, we next analyzed the effects of Qki down-regulation on neuronal development. Hippocampal neurons were infected with lentivirus expressing short hairpin RNAs (shRNAs) against *Qki* (sh-Qki-1, -2, and -3) (Fig. 6, *A* and *B*), and dendritic formation was evaluated. We first checked the knockdown efficiency of sh-Qki-1 by immuno-

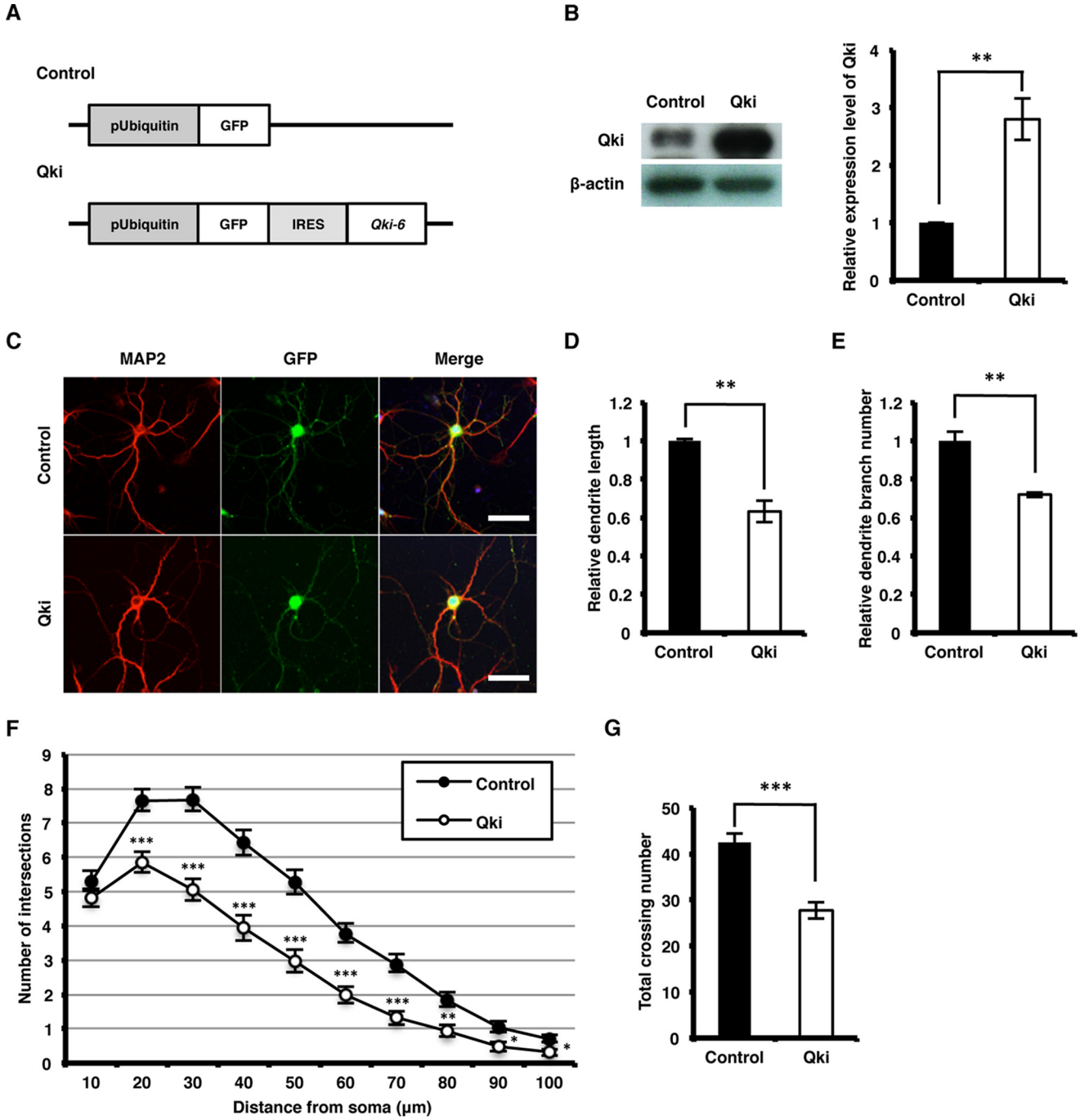

FIGURE 5. **Overexpression of Qki suppresses dendritic development in hippocampal neurons.** *A*, diagrams of lentiviral vector constructs. GFP only or GFP together with Qki are expressed under the ubiquitin promoter. *B*, representative immunoblots (*left*) and quantitative data (*right*) of Qki. Qki protein levels were analyzed by immunoblotting with anti-Qki antibody in neurons infected with control or *Qki*-expressing lentiviruses. Student's *t* test, **, $p < 0.01$. $n = 3$ independent experiments. *C*, representative images of hippocampal neurons, stained with anti-MAP2 (*red*) and anti-GFP (*green*) antibodies at 6DIV. *Scale bars,* 50 μm. *D* and *E*, quantification of dendrite number (*D*) and total dendrite length (*E*) in *C*. Student's *t* test, **, $p < 0.01$. $n = 3$ independent experiments; at least 50 neurons were analyzed in each experiment. *F*, quantification of dendrite complexity by Sholl analysis of neurons infected with lentiviruses expressing *Qki* at 6DIV. Student's *t* test, *, $p < 0.05$; **, $p < 0.01$; ***, $p < 0.001$. 50 neurons were analyzed in each condition. *G*, histogram of total number of crossing for Qki-expressing neurons. Student's *t* test, ***, $p < 0.001$.

blotting analysis and observed a marked reduction of Qki protein levels following the expression of the shRNA (Fig. 6*C*). Knockdown of *Qki* increased dendritic numbers and total dendrite length (Fig. 6, *D–F*). Dendritic complexity was also increased by *Qki* knockdown (Fig. 6, *G* and *H*). We repeated the same experiments with an additional two shRNAs for *Qki* (sh-Qki-2 and -3) with different target sequences and obtained almost the same results (Fig. 6, *B* and *I–N*). These results suggest that Qki is important for dendritic elaboration in neurons.

Qki Acts Downstream of miR-214 in Dendritic Development—If miR-214 influences dendritic development by regulating Qki, expression of Qki should cancel the effects of miR-214. To test this prediction, we co-expressed miR-214 with *Qki*, either pos-

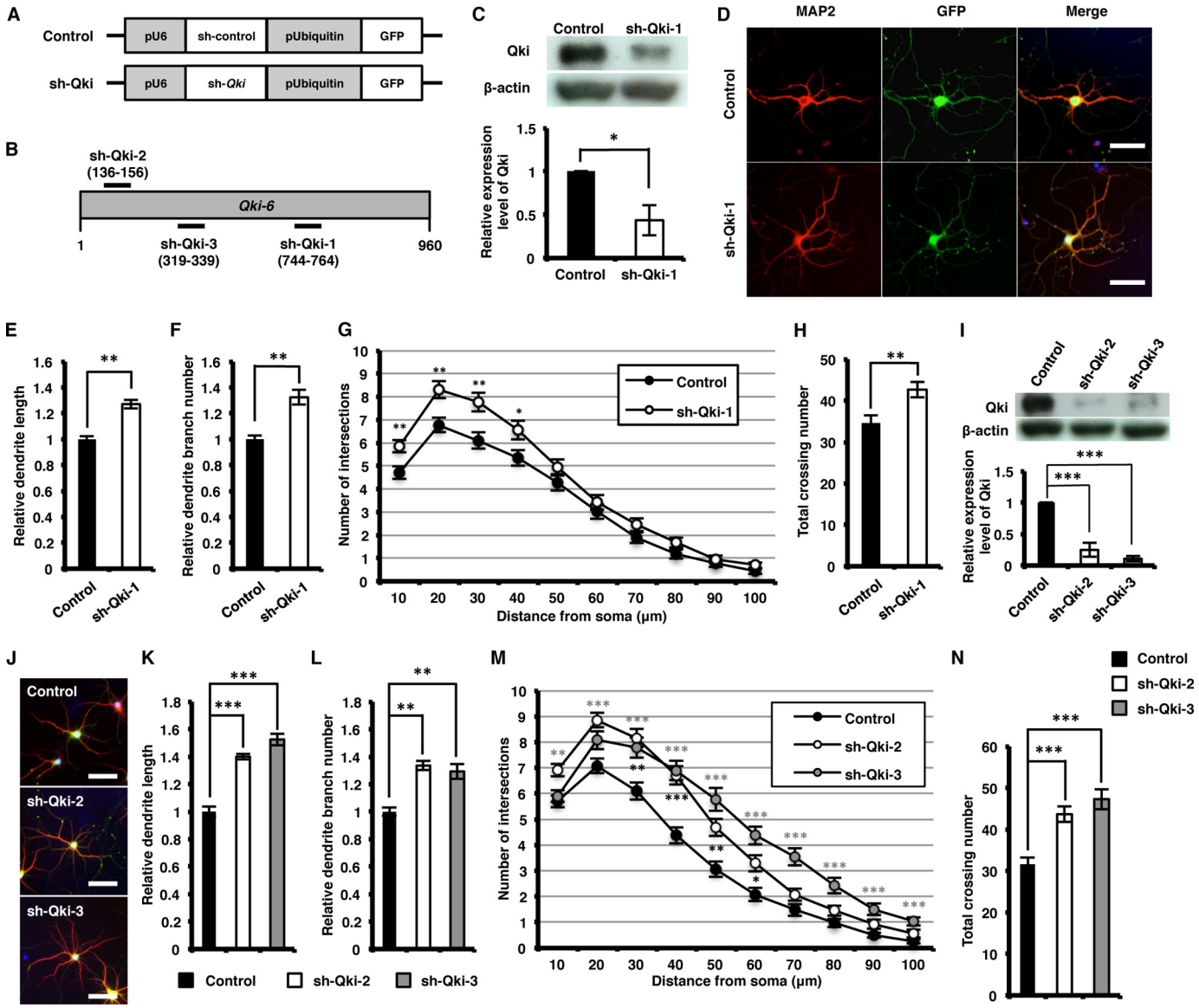

FIGURE 6. **Knockdown of Qki promotes dendritic development in hippocampal neurons.** *A*, diagrams of lentiviral vector constructs. shRNA is expressed under the U6 RNA polymerase III promoter, and GFP is expressed under the ubiquitin promoter. *B*, schematic image for the location of shRNAs for *Qki-6*. *C*, representative immunoblots (*left*) and quantitative data (*right*) of Qki. Qki protein levels were analyzed by immunoblotting with anti-Qki antibody in neurons infected with lentivirus expressing shRNA against *Qki* (*sh-Qki-1*). Student's *t* test, *, $p < 0.05$. $n = 3$ independent experiments. *D*, representative images of hippocampal neurons, stained with anti-MAP2 (*red*) and anti-GFP (*green*) antibodies at 6DIV. *Scale bars*, 50 μm. *E* and *F*, quantification of total dendrite length (*E*) and dendrite branch number (*F*) in *D*. Student's *t* test, **, $p < 0.01$. $n = 3$ independent experiments; at least 50 neurons were analyzed in each experiment. *G*, quantification of dendrite complexity by Sholl analysis of neurons infected with lentiviruses expressing shRNA against *Qki* at 6DIV. Student's *t* test, *, $p < 0.05$; **, $p < 0.01$. 50 neurons were analyzed in each condition. *H*, histogram of total number of crossings for shRNA against *Qki*-expressing neurons. Student's *t* test, **, $p < 0.01$. *I*, representative immunoblots and quantitative data of Qki. Qki protein levels were analyzed by immunoblotting with anti-Qki antibody in neurons infected with lentivirus expressing the other 2 shRNAs against *Qki* (sh-Qki-2 and -3). One-way ANOVA, Tukey's post-test, ***, $p < 0.001$. $n = 3$ independent experiments. *J*, representative images of hippocampal neurons, stained with anti-MAP2 (*red*) and anti-GFP (*green*) antibodies at 6DIV. *Scale bars*, 50 μm. *K* and *L*, quantification of total dendrite length (*K*) and dendrite branch number (*L*) in *J*. One-way ANOVA, Tukey's post-test, **, $p < 0.01$; ***, $p < 0.001$. $n = 3$ independent experiments; at least 50 neurons were analyzed in each experiment. *M*, quantification of dendrite complexity by Sholl analysis of neurons infected at 6DIV with lentiviruses expressing sh-Qki-2 and -3. One-way ANOVA, Tukey's post-test, *, $p < 0.05$; **, $p < 0.01$; ***, $p < 0.001$. 50 neurons were analyzed. *N*, histogram of total number of crossing for sh-Qki-2- and -3-expressing neurons. One-way ANOVA, Tukey's post-test, ***, $p < 0.001$.

sessing or lacking its 3′UTR containing three miR-214 target sites, in hippocampal neurons (Fig. 7*A*) and assessed dendrite morphology. The expression levels of miR-214 and Qki in lentivirus-infected neurons were confirmed by qRT-PCR and immunoblotting, respectively (Fig. 7, *B* and *C*). We found that co-expression with *Qki* abrogated the enhanced dendritic growth induced by the expression of miR-214 (Fig. 7, *D–F*). The effects of miR-214 on dendritic complexity were also diminished by *Qki* expression (Fig. 7*G*). The total number of dendrite crossings in Qki-co-expressing neurons showed abrogation of the increased dendrite complexity by miR-214 expression (Fig. 7*H*). When *Qki* possessing its 3′UTR sequence (Qki-3′UTR) was co-expressed with miR-214, abrogation of miR-214 function in dendritic formation was less effective (Fig. 7, *D–H*). Together, these data indicate that Qki acts downstream of miR-214 in the regulation of dendritic development in hippocampal neurons.

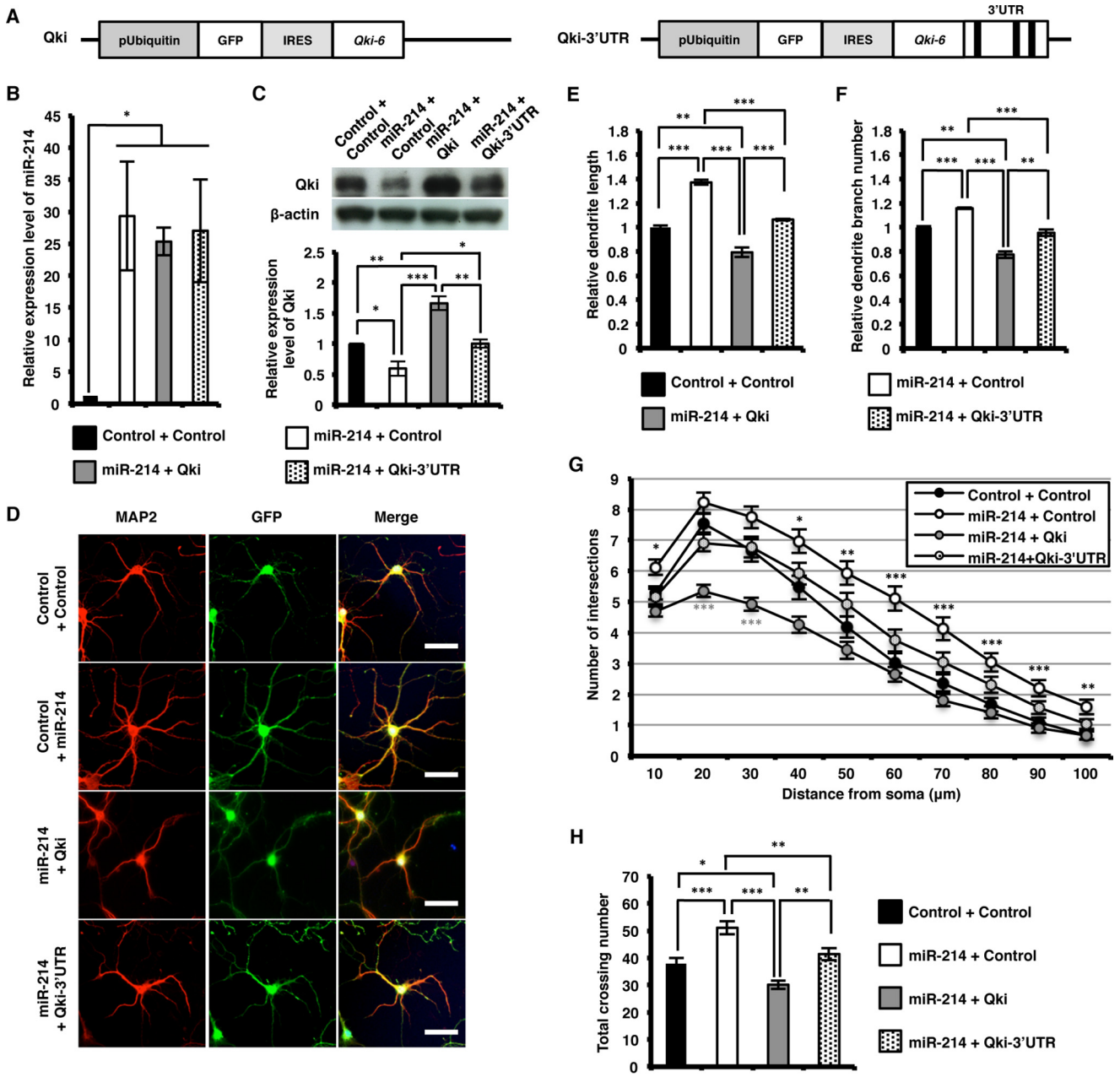

FIGURE 7. **Overexpression of Qki abolishes the effect of miR-214 in hippocampal neurons.** *A*, schematic diagrams of lentiviral vector constructs expressing *Qki* and *Qki* fused with its 3′UTR containing miR-214 target sites (*black bars*). *B*, expression levels of miR-214 were measured by qRT-PCR in hippocampal neurons co-infected with lentiviruses expressing miR-214 and either *Qki* or *Qki* fused with its 3′UTR. One-way ANOVA, Dunnett's post-test, *, $p < 0.05$. $n = 3$ independent experiments. *C*, representative immunoblots (*upper*) and quantitative data (*bottom*) of Qki. Qki protein levels were analyzed by immunoblotting with anti-Qki antibody in neurons infected with miR-214-expressing lentivirus together with lentivirus expressing Qki or Qki fused with its 3′UTR. One-way ANOVA, Tukey's post-test, *, $p < 0.05$; **, $p < 0.01$; ***, $p < 0.001$. $n = 3$ independent experiments. *D*, representative images of hippocampal neurons, stained with anti-MAP2 (*red*) and anti-GFP (*green*) antibodies at 6DIV. *Scale bars,* 50 μm. *E* and *F*, quantification of total dendrite length (*E*) and dendrite branch number (*F*) in *D*. One-way ANOVA, Tukey's post-test, **, $p < 0.01$; ***, $p < 0.001$. $n = 3$ independent experiments; at least 50 neurons were analyzed in each experiment. *G*, quantification of dendrite complexity by Sholl analysis of neurons infected at 6DIV with lentiviruses co-expressing miR-214 and either *Qki* or *Qki* fused with its 3′UTR. One-way ANOVA, Tukey's post-test, *, $p < 0.05$; **, $p < 0.01$; ***, $p < 0.001$. 60 neurons were analyzed in each condition. *H*, histogram of total crossing number of neurons co-expressing miR-214 and either *Qki* or *Qki* fused with its 3′UTR. One-way ANOVA, Tukey's post-test, *, $p < 0.05$; **, $p < 0.01$; ***, $p < 0.001$.

miR-214 and Qki Affect Dendritic Growth in Vivo—To confirm the effects of miR-214 and Qki on dendritic growth *in vivo*, we introduced constructs expressing GFP alone (control) or GFP together with miR-214 or Qki into embryonic cerebral cortices by *in utero* electroporation at E14, and the brains were fixed at P10. Almost all of the transduced cells were situated in layer 2/3–4 (Fig. 8*A*). Expression of miR-214 significantly increased total dendrite length and branch number compared with control (Fig. 8, *B–E*). Sholl analysis also revealed that overexpression of miR-214 promoted dendritic arborization (Fig. 8*F*). In addition, the total number of crossings was increased in miR-214-expressing neurons (Fig. 8*G*). In contrast, expression of Qki clearly suppressed dendritic formation compared with control (Fig. 8, *B–E*). Dendritic complexity was also decreased by Qki expression (Fig. 8, *F* and *G*). Taken together, these results suggest that the miR-214-Qki pathway regulates dendritic development *in vivo*.

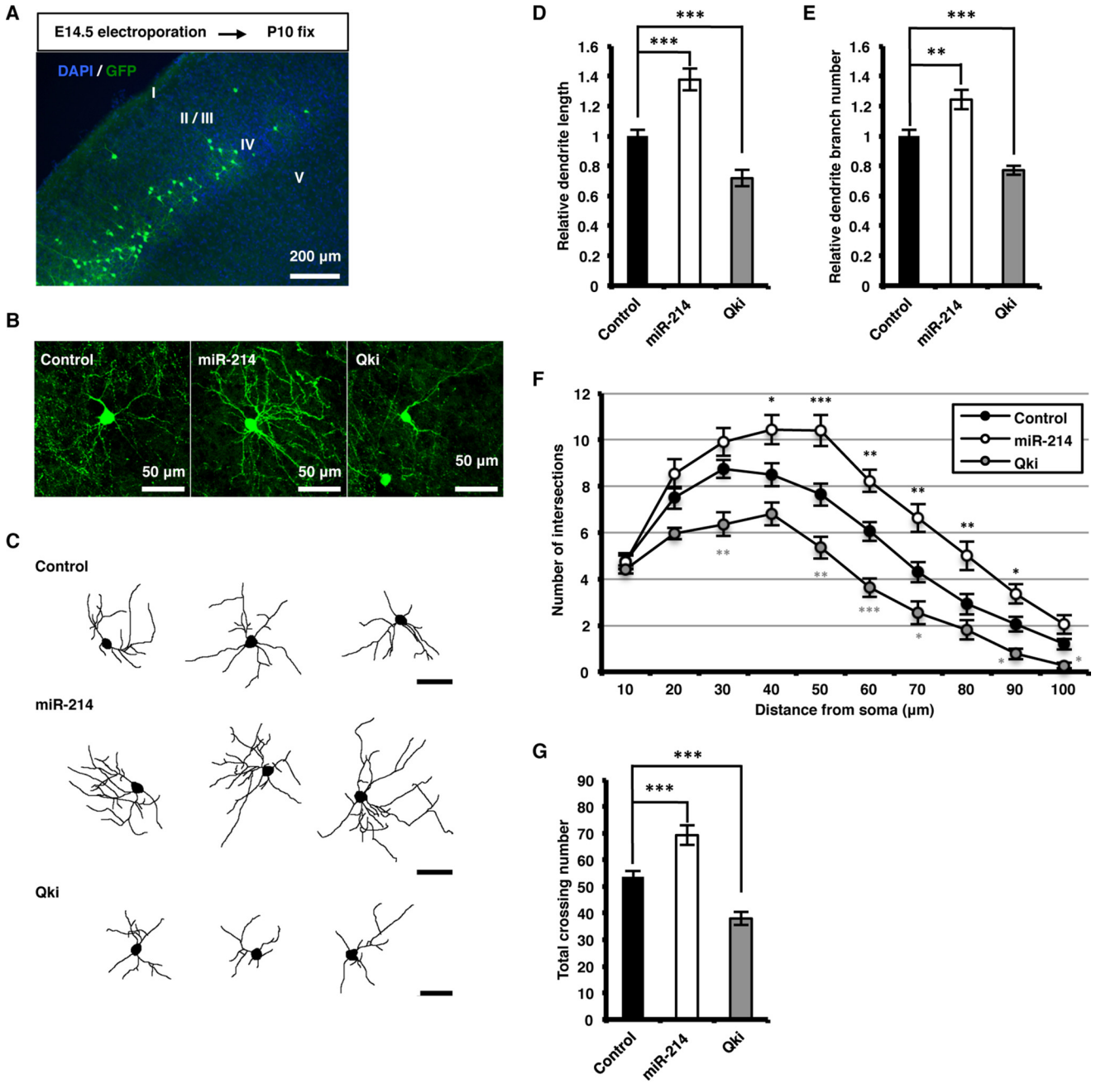

FIGURE 8. **miR-214 and Qki affect dendritic growth *in vivo*.** *A*, representative image of a transfected brain section stained with anti-GFP antibody. Mouse embryos were transfected with plasmids expressing only GFP (*control*), or GFP together with miR-214 (*miR-214*) or *Qki* (*Qki*) by *in utero* electroporation at E14 and sacrificed at P10. *Scale bar,* 200 μm. *B*, representative images of transfected neurons, stained with anti-GFP antibodies at P10. *Scale bars,* 50 μm. *C*, representative tracing images of neurons transfected with the constructs as in *B*. *Scale bars,* 50 μm. *D* and *E*, quantification of total dendrite length (*D*) and dendrite branch number (*E*) in *C*. One-way ANOVA, Tukey's post-test, **, $p < 0.01$; ***, $p < 0.001$. Number of cells analyzed; *control*, 36 neurons from nine brains; *miR-214,* 22 neurons from five brains; *Qki,* 22 neurons from five brains. *F*, quantification of dendrite complexity by Sholl analysis of neurons in *C*. One-way ANOVA, Tukey's post-test, *, $p < 0.05$; **, $p < 0.01$; ***, $p < 0.001$. Number of cells analyzed; *control*, 36 neurons from nine brains; *miR-214.* 22 neurons from five brains; *Qki,* 22 neurons from five brains. *G*, histogram of total number of crossing for miR-214- or Qki-expressing neurons. One-way ANOVA, Tukey's post-test, ***, $p < 0.001$.

Discussion

As dendrites are the main site of synaptic input into neurons, the structure of the dendrite branch and the targeting of dendrites into appropriate territories are critical determinants of the input properties of neurons. Therefore, the regulation of dendritic morphogenesis is crucial for the establishment of functional neuronal circuits, and dysregulation of dendrite formation may be a cause of neurological diseases such as psychiatric disorders (4, 5, 38, 39).

Recent research has revealed that miRNAs act as regulators of many aspects of neuronal development such as neuronal differentiation, neuronal outgrowth, and dendritic spine morphogenesis (11, 40–42). Although it has recently been reported that miR-137 negatively regulates aspects of neuronal maturation, including dendritic formation (13), the role of miRNA in dendrite development remains poorly understood.

In this study, we investigated the functional role of miR-214 in primary cultured hippocampal neurons. We observed a tran-

sient up-regulation of primary miR-214 expression at an early stage in the development of hippocampal neurons in culture, and its expression decreased at later stages. In contrast, the level of mature miR-214 gradually increased during neuronal maturation. These observations made us think that miR-214 might play a role in neuronal maturation and also suggested that the abundance of mature miR-214 is tightly controlled at the post-transcriptional level during neuronal maturation. Here, we demonstrated that overexpression of miR-214 increases total dendritic length, branch numbers, and dendritic complexity. We also showed that loss of miR-214 function inhibits dendritic arborization. These data clearly indicate that miR-214 positively controls dendritic development.

Identifying downstream mRNA targets is essential to understand the function of miRNAs. By performing database searches and functional screening, we identified *Qki* as a candidate target gene of miR-214. Qki governs post-transcriptional regulation of its mRNA ligands by regulating pre-mRNA splicing (43, 44), mRNA turnover (45), and translation (46). Qki has also been shown to regulate cellular processes, including apoptosis, the cell cycle, and development (47, 48). In particular, Qki is involved in oligodendrocyte development and myelination (49, 50) in the central nervous system. However, the function of Qki in neurons has not yet been investigated. In this study, we demonstrated that overexpression and knockdown of *Qki* impeded and enhanced dendritic morphogenesis, respectively, suggesting that Qki negatively regulates dendritic formation. The finding that Qki abolishes dendritic phenotypes induced by the expression of miR-214 further supports the negative effects of Qki on dendritic development and its role as a downstream effector of miR-214. Although Qki clearly functions downstream of miR-214, database searches identified other predicted miR-214 targets, and we therefore cannot rule out the possibility that miR-214 can modulate the expression of these genes. Further experiments to identify additional miR-214 targets will give us more insight into the molecular function of miR-214 during neuronal development.

How does Qki regulate dendritic development? Previous work has identified many putative mRNA targets of Qki, using SELEX (systematic evolution of ligands by exponential enrichment) and bioinformatic analysis (51). Interestingly, among these candidate targets are *Wnt2a* and *Rab5a*. The Wnt-dishevelled pathway regulates dendrite morphogenesis in mammalian neurons, whereas Rab5, a component of the early endocytic pathway, promotes dendritic branching of fly dendritic arborization neurons (6). Thus, it is plausible that Qki controls dendrite development by regulating these mRNAs. In addition, because actin is one of the major structural components that underlie dendrite morphology, regulators of actin are implicated in dendrite morphogenesis. Another study showed that Qki regulates actin-interacting protein-1 (*AIP1*) mRNA stability during oligodendrocyte differentiation (52). Thus, it is possible that Qki also targets *AIP1* in neurons, thereby regulating dendritic morphogenesis. It will be of interest to determine how Qki controls dendritic development in future studies.

Multiple studies have implicated QKI in schizophrenia (37, 53). Furthermore, it is known that altered dendritic morphology contributes to various neurological disorders, including

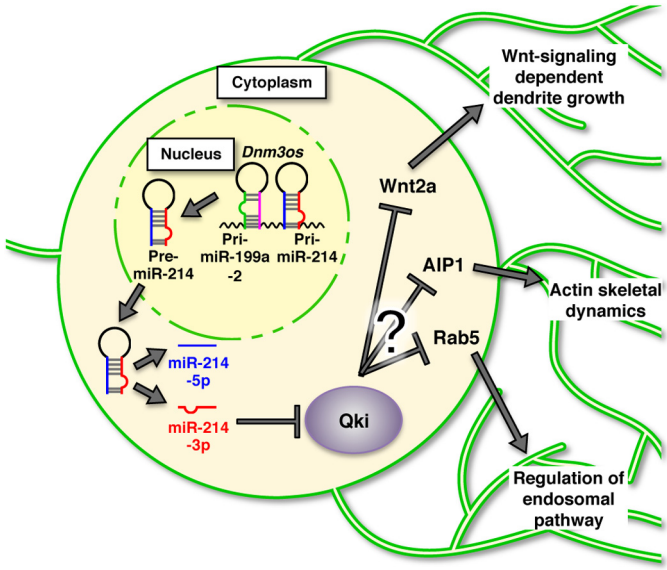

FIGURE 9. **Model of the regulation of dendritic development by the miR-214-Qki pathway.** pre-miR-214 is processed from pri-miR-214 (*Dnm3os*). pre-miR-214 is further processed into mature miR-214–5p and -3p. miR-214-3p binds to the *Qki* 3′UTR and suppresses the expression of Qki, a protein that negatively regulates dendritic development in hippocampal neurons. Consequently, miR-214 promotes dendritic growth in hippocampal neurons.

schizophrenia (54–56). Here, we described an important function of miR-214 in dendritic growth as a regulator of Qki expression in hippocampal neurons. Thus, it is possible that impairments of dendritic development by miR-214-Qki pathway dysfunction lead to the abnormal dendritic phenotypes observed in psychiatric diseases. Given our demonstration that miR-214 targets *Qki*, it will be intriguing to explore further whether miR-214 is a candidate susceptibility gene for major mental illness, and whether miR-214 knock-out mice show any of behavioral abnormalities associated with psychiatric diseases.

Taken together, our findings uncover an important role for the miR-214-Qki pathway in dendritic development (Fig. 9). We anticipate that elucidating this pathway in more detail will also contribute to a deeper understanding of the molecular mechanisms underlying neuropsychiatric disorders such as schizophrenia.

Author Contributions—K. I. performed all of the experiments with support from H. N. K. T. conceived and designed the research. K. I., K. T., and K. N. wrote the manuscript. K. N. coordinated and supervised the study. All authors reviewed and approved the final version of the manuscript.

Acknowledgments—We thank M. E. Greenberg and Z. Zhou for sharing reagents, I. Smith for editing the manuscript, and all members of the Laboratory of Molecular Neuroscience, Department of Stem Cell Biology and Medicine, Kyushu University. We appreciate the technical assistance from the Research Support Center, Research Center for Human Disease Modeling, Kyushu University Graduate School of Medical Sciences.

References

1. Craig, A. M., and Banker, G. (1994) Neuronal polarity. *Annu. Rev. Neurosci.* **17,** 267–310

2. Hume, R. I., and Purves, D. (1981) Geometry of neonatal neurones and the regulation of synapse elimination. *Nature* **293,** 469–471
3. Snider, W. D. (1987) The dendritic complexity and innervation of submandibular neurons in five species of mammals. *J. Neurosci.* **7,** 1760–1768
4. Parrish, J. Z., Emoto, K., Jan, L. Y., and Jan, Y. N. (2007) Polycomb genes interact with the tumor suppressor genes hippo and warts in the maintenance of *Drosophila* sensory neuron dendrites. *Genes Dev.* **21,** 956–972
5. Spruston, N. (2008) Pyramidal neurons: dendritic structure and synaptic integration. *Nat. Rev. Neurosci.* **9,** 206–221
6. Jan, Y. N., and Jan, L. Y. (2010) Branching out: mechanisms of dendritic arborization. *Nat. Rev. Neurosci.* **11,** 316–328
7. Siomi, H., and Siomi, M. C. (2010) Posttranscriptional regulation of microRNA biogenesis in animals. *Mol. Cell* **38,** 323–332
8. Winter, J., Jung, S., Keller, S., Gregory, R. I., and Diederichs, S. (2009) Many roads to maturity: microRNA biogenesis pathways and their regulation. *Nat. Cell Biol.* **11,** 228–234
9. Li, X., and Jin, P. (2010) Roles of small regulatory RNAs in determining neuronal identity. *Nat. Rev. Neurosci.* **11,** 329–338
10. Qurashi, A., and Jin, P. (2010) Small RNA-mediated gene regulation in neurodevelopmental disorders. *Curr. Psychiatry Rep.* **12,** 154–161
11. Dajas-Bailador, F., Bonev, B., Garcez, P., Stanley, P., Guillemot, F., and Papalopulu, N. (2012) microRNA-9 regulates axon extension and branching by targeting Map1b in mouse cortical neurons. *Nat. Neurosci.* **15,** 697–699
12. Siegel, G., Obernosterer, G., Fiore, R., Oehmen, M., Bicker, S., Christensen, M., Khudayberdiev, S., Leuschner, P. F., Busch, C. J., Kane, C., Hübel, K., Dekker, F., Hedberg, C., Rengarajan, B., Drepper, C., *et al.* (2009) A functional screen implicates microRNA-138-dependent regulation of the depalmitoylation enzyme APT1 in dendritic spine morphogenesis. *Nat. Cell Biol.* **11,** 705–716
13. Smrt, R. D., Szulwach, K. E., Pfeiffer, R. L., Li, X., Guo, W., Pathania, M., Teng, Z. Q., Luo, Y., Peng, J., Bordey, A., Jin, P., and Zhao, X. (2010) MicroRNA miR-137 regulates neuronal maturation by targeting ubiquitin ligase mind bomb-1. *Stem. Cells* **28,** 1060–1070
14. Liu, J., Luo, X. J., Xiong, A. W., Zhang, Z. D., Yue, S., Zhu, M. S., and Cheng, S. Y. (2010) MicroRNA-214 promotes myogenic differentiation by facilitating exit from mitosis via down-regulation of proto-oncogene N-ras. *J. Biol. Chem.* **285,** 26599–26607
15. Xu, C. X., Xu, M., Tan, L., Yang, H., Permuth-Wey, J., Kruk, P. A., Wenham, R. M., Nicosia, S. V., Lancaster, J. M., Sellers, T. A., and Cheng, J. Q. (2012) MicroRNA miR-214 regulates ovarian cancer cell stemness by targeting p53/Nanog. *J. Biol. Chem.* **287,** 34970–34978
16. Aurora, A. B., Mahmoud, A. I., Luo, X., Johnson, B. A., van Rooij, E., Matsuzaki, S., Humphries, K. M., Hill, J. A., Bassel-Duby, R., Sadek, H. A., and Olson, E. N. (2012) MicroRNA-214 protects the mouse heart from ischemic injury by controlling Ca^{2+} overload and cell death. *J. Clin. Invest.* **122,** 1222–1232
17. Chen, H., Shalom-Feuerstein, R., Riley, J., Zhang, S. D., Tucci, P., Agostini, M., Aberdam, D., Knight, R. A., Genchi, G., Nicotera, P., Melino, G., and Vasa-Nicotera, M. (2010) miR-7 and miR-214 are specifically expressed during neuroblastoma differentiation, cortical development and embryonic stem cells differentiation, and control neurite outgrowth *in vitro*. *Biochem. Biophys. Res. Commun.* **394,** 921–927
18. Justice, M. J., and Bode, V. C. (1988) Three ENU-induced alleles of the murine quaking locus are recessive embryonic lethal mutations. *Genet Res.* **51,** 95–102
19. Sidman, R. L., Dickie, M. M., and Appel, S. H. (1964) Mutant mice (Quaking and Jimpy) with deficient myelination in the central nervous system. *Science* **144,** 309–311
20. Kaech, S., and Banker, G. (2006) Culturing hippocampal neurons. *Nat. Protoc.* **1,** 2406–2415
21. Lois, C., Hong, E. J., Pease, S., Brown, E. J., and Baltimore, D. (2002) Germline transmission and tissue-specific expression of transgenes delivered by lentiviral vectors. *Science* **295,** 868–872
22. Zhou, Z., Hong, E. J., Cohen, S., Zhao, W. N., Ho, H. Y., Schmidt, L., Chen, W. G., Lin, Y., Savner, E., Griffith, E. C., Hu, L., Steen, J. A., Weitz, C. J., and Greenberg, M. E. (2006) Brain-specific phosphorylation of MeCP2 regulates activity-dependent Bdnf transcription, dendritic growth, and spine maturation. *Neuron* **52,** 255–269
23. Tsujimura, K., Irie, K., Nakashima, H., Egashira, Y., Fukao, Y., Fujiwara, M., Itoh, M., Uesaka, M., Imamura, T., Nakahata, Y., Yamashita, Y., Abe, T., Takamori, S., and Nakashima, K. (2015) miR-199a links MeCP2 with mTOR signaling and its dysregulation leads to Rett syndrome phenotypes. *Cell Rep.* **12,** 1887–1901
24. Kawauchi, T., Sekine, K., Shikanai, M., Chihama, K., Tomita, K., Kubo, K., Nakajima, K., Nabeshima, Y., and Hoshino, M. (2010) Rab GTPases-dependent endocytic pathways regulate neuronal migration and maturation through *N*-cadherin trafficking. *Neuron* **67,** 588–602
25. Zagrebelsky, M., Holz, A., Dechant, G., Barde, Y. A., Bonhoeffer, T., and Korte, M. (2005) The p75 neurotrophin receptor negatively modulates dendrite complexity and spine density in hippocampal neurons. *J. Neurosci.* **25,** 9989–9999
26. Suzuki, H. I., Yamagata, K., Sugimoto, K., Iwamoto, T., Kato, S., and Miyazono, K. (2009) Modulation of microRNA processing by p53. *Nature* **460,** 529–533
27. Ebersole, T. A., Chen, Q., Justice, M. J., and Artzt, K. (1996) The quaking gene product necessary in embryogenesis and myelination combines features of RNA binding and signal transduction proteins. *Nat. Genet.* **12,** 260–265
28. Zhao, L., Ku, L., Chen, Y., Xia, M., LoPresti, P., and Feng, Y. (2006) QKI binds MAP1B mRNA and enhances MAP1B expression during oligodendrocyte development. *Mol. Biol. Cell* **17,** 4179–4186
29. Aberg, K., Saetre, P., Lindholm, E., Ekholm, B., Pettersson, U., Adolfsson, R., and Jazin, E. (2006) Human QKI, a new candidate gene for schizophrenia involved in myelination. *Am. J. Med. Genet. B Neuropsychiatr. Genet.* **141B,** 84–90
30. Lindholm, E., Ekholm, B., Shaw, S., Jalonen, P., Johansson, G., Pettersson, U., Sherrington, R., Adolfsson, R., and Jazin, E. (2001) A schizophrenia-susceptibility locus at 6q25, in one of the world's largest reported pedigrees. *Am. J. Hum. Genet.* **69,** 96–105
31. Lewis, C. M., Levinson, D. F., Wise, L. H., DeLisi, L. E., Straub, R. E., Hovatta, I., Williams, N. M., Schwab, S. G., Pulver, A. E., Faraone, S. V., Brzustowicz, L. M., Kaufmann, C. A., Garver, D. L., Gurling, H. M., Lindholm, E., *et al.* (2003) Genome scan meta-analysis of schizophrenia and bipolar disorder, part II: Schizophrenia. *Am. J. Hum. Genet.* **73,** 34–48
32. Fanous, A. H., Neale, M. C., Webb, B. T., Straub, R. E., Amdur, R. L., O'Neill, F. A., Walsh, D., Riley, B. P., and Kendler, K. S. (2007) A genome-wide scan for modifier loci in schizophrenia. *Am. J. Med. Genet. B Neuropsychiatr. Genet.* **144B,** 589–595
33. Ng, M. Y., Levinson, D. F., Faraone, S. V., Suarez, B. K., DeLisi, L. E., Arinami, T., Riley, B., Paunio, T., Pulver, A. E., Irmansyah, Holmans, P. A., Escamilla, M., Wildenauer, D. B., Williams, N. M., Laurent, C., Mowry, B. J., *et al.* (2009) Meta-analysis of 32 genome-wide linkage studies of schizophrenia. *Mol. Psychiatry* **14,** 774–785
34. Aberg, K., Saetre, P., Jareborg, N., and Jazin, E. (2006) Human QKI, a potential regulator of mRNA expression of human oligodendrocyte-related genes involved in schizophrenia. *Proc. Natl. Acad. Sci. U.S.A.* **103,** 7482–7487
35. Haroutunian, V., Katsel, P., Dracheva, S., and Davis, K. L. (2006) The human homolog of the QKI gene affected in the severe dysmyelination "quaking" mouse phenotype: downregulated in multiple brain regions in schizophrenia. *Am. J. Psychiatry* **163,** 1834–1837
36. McCullumsmith, R. E., Gupta, D., Beneyto, M., Kreger, E., Haroutunian, V., Davis, K. L., and Meador-Woodruff, J. H. (2007) Expression of transcripts for myelination-related genes in the anterior cingulate cortex in schizophrenia. *Schizophr. Res.* **90,** 15–27
37. Klempan, T. A., Ernst, C., Deleva, V., Labonte, B., and Turecki, G. (2009) Characterization of QKI gene expression, genetics, and epigenetics in suicide victims with major depressive disorder. *Biol. Psychiatry* **66,** 824–831
38. London, M., and Häusser, M. (2005) Dendritic computation. *Annu. Rev. Neurosci.* **28,** 503–532
39. Mumm, J. S., Williams, P. R., Godinho, L., Koerber, A., Pittman, A. J., Roeser, T., Chien, C. B., Baier, H., and Wong, R. O. (2006) *In vivo* imaging reveals dendritic targeting of laminated afferents by zebrafish retinal ganglion cells. *Neuron* **52,** 609–621
40. Schratt, G. M., Tuebing, F., Nigh, E. A., Kane, C. G., Sabatini, M. E.,

Kiebler, M., and Greenberg, M. E. (2006) A brain-specific microRNA regulates dendritic spine development. *Nature* **439,** 283–289
41. Makeyev, E. V., Zhang, J., Carrasco, M. A., and Maniatis, T. (2007) The microRNA miR-124 promotes neuronal differentiation by triggering brain-specific alternative pre-mRNA splicing. *Mol. Cell* **27,** 435–448
42. Motti, D., Bixby, J. L., and Lemmon, V. P. (2012) MicroRNAs and neuronal development. *Semin. Fetal Neonatal Med.* **17,** 347–352
43. Hall, M. P., Nagel, R. J., Fagg, W. S., Shiue, L., Cline, M. S., Perriman, R. J., Donohue, J. P., and Ares, M., Jr. (2013) Quaking and PTB control overlapping splicing regulatory networks during muscle cell differentiation. *RNA* **19,** 627–638
44. Wu, J. I., Reed, R. B., Grabowski, P. J., and Artzt, K. (2002) Function of quaking in myelination: regulation of alternative splicing. *Proc. Natl. Acad. Sci. U.S.A.* **99,** 4233–4238
45. Larocque, D., and Richard, S. (2005) QUAKING KH domain proteins as regulators of glial cell fate and myelination. *RNA Biol.* **2,** 37–40
46. Saccomanno, L., Loushin, C., Jan, E., Punkay, E., Artzt, K., and Goodwin, E. B. (1999) The STAR protein QKI-6 is a translational repressor. *Proc. Natl. Acad. Sci. U.S.A.* **96,** 12605–12610
47. Li, Z., Takakura, N., Oike, Y., Imanaka, T., Araki, K., Suda, T., Kaname, T., Kondo, T., Abe, K., and Yamamura, K. (2003) Defective smooth muscle development in qkI-deficient mice. *Dev. Growth Differ.* **45,** 449–462
48. Pilotte, J., Larocque, D., and Richard, S. (2001) Nuclear translocation controlled by alternatively spliced isoforms inactivates the QUAKING apoptotic inducer. *Genes Dev.* **15,** 845–858
49. Larocque, D., Galarneau, A., Liu, H. N., Scott, M., Almazan, G., and Richard, S. (2005) Protection of p27(Kip1) mRNA by quaking RNA binding proteins promotes oligodendrocyte differentiation. *Nat. Neurosci.* **8,** 27–33
50. Larocque, D., Pilotte, J., Chen, T., Cloutier, F., Massie, B., Pedraza, L., Couture, R., Lasko, P., Almazan, G., and Richard, S. (2002) Nuclear retention of MBP mRNAs in the quaking viable mice. *Neuron* **36,** 815–829
51. Galarneau, A., and Richard, S. (2005) Target RNA motif and target mRNAs of the Quaking STAR protein. *Nat. Struct. Mol. Biol.* **12,** 691–698
52. Doukhanine, E., Gavino, C., Haines, J. D., Almazan, G., and Richard, S. (2010) The QKI-6 RNA binding protein regulates actin-interacting protein-1 mRNA stability during oligodendrocyte differentiation. *Mol. Biol. Cell* **21,** 3029–3040
53. Chénard, C. A., and Richard, S. (2008) New implications for the QUAKING RNA binding protein in human disease. *J. Neurosci. Res.* **86,** 233–242
54. Rosoklija, G., Toomayan, G., Ellis, S. P., Keilp, J., Mann, J. J., Latov, N., Hays, A. P., and Dwork, A. J. (2000) Structural abnormalities of subicular dendrites in subjects with schizophrenia and mood disorders: preliminary findings. *Arch. Gen. Psychiatry* **57,** 349–356
55. Soetanto, A., Wilson, R. S., Talbot, K., Un, A., Schneider, J. A., Sobiesk, M., Kelly, J., Leurgans, S., Bennett, D. A., and Arnold, S. E. (2010) Association of anxiety and depression with microtubule-associated protein 2- and synaptopodin-immunolabeled dendrite and spine densities in hippocampal CA3 of older humans. *Arch. Gen. Psychiatry* **67,** 448–457
56. Kulkarni, V. A., and Firestein, B. L. (2012) The dendritic tree and brain disorders. *Mol. Cell. Neurosci.* **50,** 10–20

MicroRNA-214 Promotes Dendritic Development by Targeting the Schizophrenia-associated Gene Quaking (*Qki*)

Koichiro Irie, Keita Tsujimura, Hideyuki Nakashima and Kinichi Nakashima

J. Biol. Chem. 2016, 291:13891-13904.
doi: 10.1074/jbc.M115.705749 originally published online April 28, 2016